Understanding the Response of Composite Structures to Fire

ASIF S. USMANI

This paper was presented at the 2003 North American Steel Construction Conference.

This paper is based upon research undertaken at the University of Edinburgh over the last six years after a series of full-scale fire tests had been completed on an 8-story steel frame composite building in Cardington (United Kingdom) in 1996 (University of Edinburgh, 2000; Sanad, Lamont, Usmani, and Rotter, 2000a; Sanad, Lamont, Usmani, and Rotter, 2000b; Sanad, Rotter, Usmani, and O'Connor, 2000c; Gillie, Usmani, and Rotter, 2001; Gillie, Usmani, and Rotter, 2002; Usmani, Rotter, Lamont, Sanad, and Gillie, 2001; Lamont, Lane, Usmani, and Drysdale, 2002; Usmani, Chung, and Torero, 2003; Lamont and Usmani, 2003). The initial work was mainly of a computational nature and progressed very slowly at first as severe geometric and material non-linearities made the analyses very difficult. This was exacerbated by our lack of sufficient understanding of the fundamental mechanics governing this problem. It was found necessary to return to first principles in order to understand the complex interactions of the different structural mechanisms taking place. This led to the development of a number of important principles that were found to govern the global behavior (Usmani and others, 2001). These principles are very useful in interpreting the results from much larger and sophisticated computational models and in helping to develop a coherent picture of the structural response. A brief review of this work and more recent developments will be presented in this paper. The Cardington tests and the subsequent research they inspired had many positive implications towards furthering the case of *performance-based design* in this field.

Behavior of composite structures in fire has long been understood to be dominated by the effects of strength loss caused by thermal degradation and consequent large deflections and runaway failure resulting from the action of imposed loading on a *weakened* structure. Thus *strength* and *loads* are quite generally believed to be the key factors determining structural response (fundamentally no different from ambient behavior). Considerable recent research in the United Kingdom and Europe shows that composite-framed structures possess enormous reserves of strength through adopting large displacement configurations (University of Edinburgh, 2000; Gillie and others, 2002; Lamont and others, 2002). This research also shows that thermally-induced forces and displacements dominate the structural response in fire (until close to failure when material degradation and loads begin to govern once again). Furthermore, it shows that material softening (such as steel yielding and buckling) can even be helpful in developing the large displacement load-carrying modes safely. This is consistent with the robust behavior seen in composite steel frame structures as demonstrated, for instance, by the Cardington tests.

The response of composite frame building structures to conventional loading is a poor guide to understanding their response to thermal loading (usually from accidental fire events). Although the same fundamental principles of structural mechanics govern all behavior, the behavior of structures under fire is often misinterpreted, even by professionals. This situation exists primarily because traditionally structures have been *protected* against fire, rather than *designed to resist* fire based on thorough understanding of behavior. Furthermore the fire protection applied is based on testing single elements in conditions that do not represent those that may actually exist in a real structure, either in terms of the fire or the structural geometry and boundary conditions. This manner of approaching structural design for fire has inhibited the development and dissemination of the understanding of structural response to high temperatures. This naturally has lead to a whole range of alternative means of providing fire resistance to structures to remain unexplored. What is even worse is that there have been situations where this lack of appreciation of structural behavior in fire has lead to designs which while efficient for well understood forms of structural loading, have been deficient for fire, despite the high cost of the fire protection applied. Finally, it should be noted that this state-of-affairs is a unique one for fire resistance design of structures. Structural engineers understand the response of structures to other extreme loads such as wind and earth-

Asif S. Usmani, senior lecturer, school of engineering and electronics, the University of Edinburgh, the Kings Buildings, Edinburgh, United Kingdom.

quakes reasonably well. Therefore large and important structures are routinely analyzed for large displacements, material non-linearities and dynamic effects. Because of the lack of understanding and appropriate training and education, fire is almost never accounted for in this explicit manner. The current trends toward greater acceptance of *performance-based design* may help improve this situation in the medium to long term, but this would require consistent and sustained commitment from a number of professions, chiefly structural engineers and regulatory authorities.

COMPONENTS OF STRUCTURAL RESPONSE TO THERMAL LOADING

In this section we will consider the response of an individual structural member under various boundary and thermal loading conditions. The response of a structural member to thermal loading can be seen as a combination of a number of material and geometric effects that arise from heating the member. In most fire resistance calculations only the response of the material and the resulting reduction in strength and stiffness are considered important and geometric effects are often ignored. This is sometimes justified by the argument that this represents the governing condition at the ultimate limit state. This argument may hold somewhat for simple structures of a nearly determinate character, but it represents a gross simplification of the behavior when dealing with large and highly indeterminate composite frame structures. Another defense for this approach is the assumption that it is conservative. While this may be true for most large redundant structures, it is by no means always the case. Sometimes not considering the geometric effects may lead to serious consequences. Understanding the geometric effects of heating on a structure is the real key to developing a proper understanding of whole structure behavior in fire. This will remain the overriding emphasis of this paper.

The most fundamental relationship that governs the behavior of structures when subjected to thermal effects is written in terms of strains as:

$$\varepsilon_{total} = \varepsilon_{thermal} + \varepsilon_{mechanical} \tag{1}$$

The total strains govern the deformed shape of the structure based on kinematic or compatibility considerations. By contrast, the stress state in the structure (elastic or plastic) depends only on the mechanical strains. When the thermal strains are free to develop in an unrestricted manner and there are no external loads (therefore no mechanical strains) all of the thermal strains are manifested as displacements in the structure. Conversely, when the thermal strains are fully restrained (still assuming no external load) and therefore the total strains are zero, the structure will experience increasing stresses with increasing temperature but will not show any displacement.

The following sections will consider the key thermal effects on a beam member. When dealing with members it is convenient to express ideas in terms of stress and strain resultant quantities instead of stresses and strain directly. This leads to the identification of two key effects that heat transfer from fire to a structural member generates. Uniform overall heating of the whole beam member made of a highly conductive material will lead to a uniform temperature increment, ΔT, in the member. If heating takes place only on one side of a member made of relatively poorly conducting material, a thermal gradient, $T_{,y}$, will be generated.

Uniform Temperature Increment, ΔT

Heating induces thermal expansion strains, ε_T, in most structural materials. These are given by

$$\varepsilon_T = \alpha \Delta T \tag{2}$$

If a uniform temperature rise, ΔT, is applied to a simply-supported beam without axial restraint, the result will simply be an expansion or increase in length of as shown in Figure 1. Therefore the total strain, ε_t, is equal to the thermal strain and there is no mechanical strain, ε_m, which means that no stresses develop in the beam.

If the beam subjected to the uniform temperature rise, ΔT, is axially restrained (as shown in Figure 2) in this case, the total strain ε_t is zero (no displacements). This is because the thermal expansion is cancelled out by equal and opposite

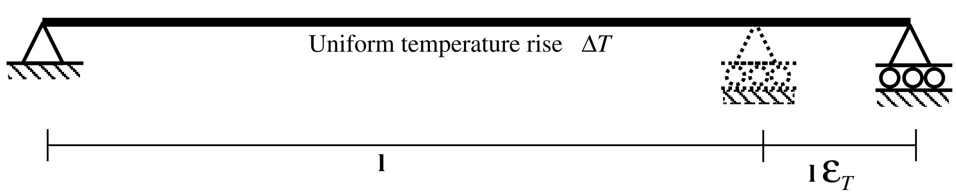

Fig. 1. Uniform heating of a simply-supported beam.

contraction caused by the restraining force P (in other words, $\varepsilon_t = \varepsilon_T + \varepsilon_m = 0$, therefore $\varepsilon_t = -\varepsilon_m$). There exists now a uniform axial stress σ in the beam equal to $E\varepsilon_m$. The magnitude of the restraining force P is therefore $-EA\alpha\Delta T$.

If the temperature is allowed to rise indefinitely, there are two basic responses, depending upon the slenderness of the beam:

1. If the beam is sufficiently stocky the axial stress will sooner or later reach the yield stress σ_y of the material. If the material has an *elastic-plastic* stress-strain relationship, the beam will continue to yield without any further increase in stress, but it will also store an increasing magnitude of *plastic* strains. The *yield temperature increment* ΔT_y is

$$\Delta T_y = \frac{\sigma_y}{E\alpha} \tag{3}$$

2. If the beam is slender then it will buckle before the material reaches its yield stress. The Euler buckling load P_{cr} for a beam-column as shown in Figure 2 is

$$P_{cr} = \frac{\pi^2 EI}{l^2} \tag{4}$$

equating this to the restraining force P (in other words, $-EA\alpha\Delta T$), leads to a critical buckling temperature of

$$\Delta T_{cr} = \frac{\pi^2}{\alpha}\left(\frac{r}{l}\right)^2 = \frac{\pi^2}{\alpha\lambda^2} \tag{5}$$

where

r = radius of gyration

λ = slenderness ratio, l/r

This expression is valid for other end-restraint conditions if l is interpreted as the *effective length*. In this case, if the temperature is allowed to rise further, the total restraining force will stay constant (assuming elastic material and no thermal degradation of properties) and the thermal expansion strains will continue to be accommodated by the outward deflection of the beam as shown in Figure 3.

The above cases represent the two fundamental responses in beams subjected to restrained thermal expansion. Either of the two (yielding or buckling) may occur on its own (based upon the slenderness of the beam) or a more complex response consisting of a combination of yielding and buckling may occur.

So far we have assumed the axial restraints to be perfectly rigid. This is an upper limit and practically impossible to achieve in real structures which offer only finite restraints. Figure 4 shows such a beam restrained axially by a translational spring of stiffness, k_t. The compressive axial stress developed by thermal expansion is

$$\sigma = \frac{EA\alpha\Delta T}{1 + \frac{EA}{k_t l}} \tag{6}$$

The critical buckling temperature is now given by

$$\Delta T_{cr} = \frac{\pi^2}{\alpha\lambda^2}\left(1 + \frac{EA}{k_t l}\right) \tag{7}$$

From Equation 7 it can be seen that buckling and post-buckling phenomena should be observable at moderate fire temperatures in structures with translational restraint stiffnesses, k_t, which are quite comparable with the axial stiffness of the member, EA/l. This can be shown very effectively by plotting the critical buckling temperature, T_{cr}, variation

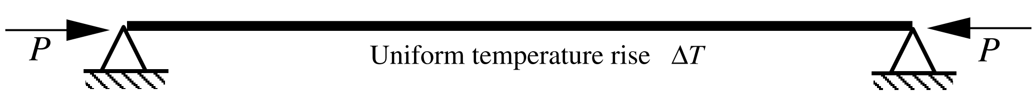

Fig. 2. Axially restrained beam subjected to uniform heating.

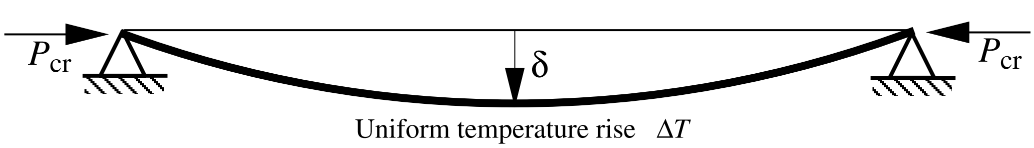

Fig. 3. Buckling of an axially restrained beam subjected to uniform heating.

against the slenderness ratio, λ, for different values of translational restraint stiffness, k_t. Figure 5 shows such a plot as derived from Equation 7. The results clearly show that the amount of restraint required is not large for slender sections to reach buckling temperature as the distance between the curves representing *infinite restraint stiffness* and restraint stiffness of the same magnitude as the member itself is not very large, particularly at high slenderness ratios. Bearing in mind that the axial stiffness of the member, *EA/l*, itself is reduced by heating because of the reduction in *E*. These facts suggest that post-buckling phenomena are very likely to be observed in beams in typical fires (University of Edinburgh, 2000).

Uniform Through-Depth Thermal Gradient, $T_{,y}$

In the previous section we discussed the effects of uniform temperature rise on axially-restrained beams. In structural members made of low conductivity materials, the surfaces exposed to fire will be at a much higher temperature than the surfaces on the opposite side. This causes the exposed surfaces to expand more than the outer surfaces inducing curvature in the member. This effect is called thermal bowing and is one of the main reasons for the deformation of concrete slabs and masonry walls in fires. Another important reason for thermal bowing in composite members is the large difference between the temperatures of the steel and concrete. This effect is much more important in the early stages of the fire when steel retains most of its strength.

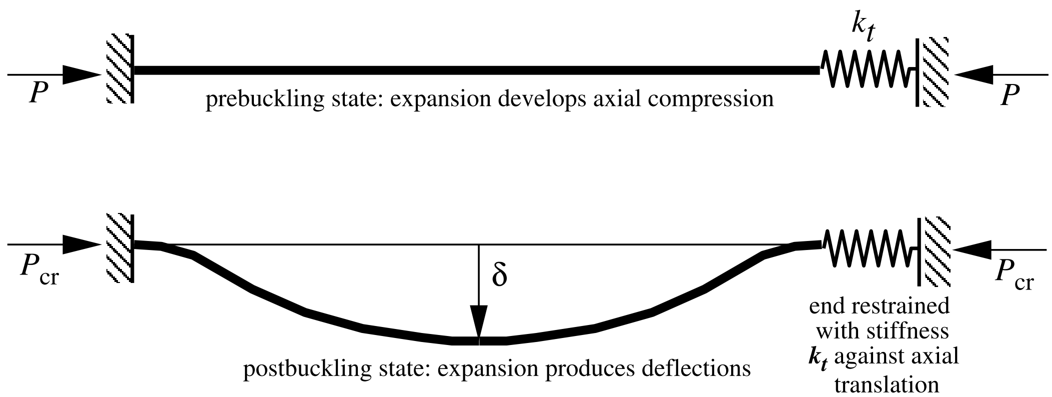

Fig. 4. Heating of beam with finite axial restraint.

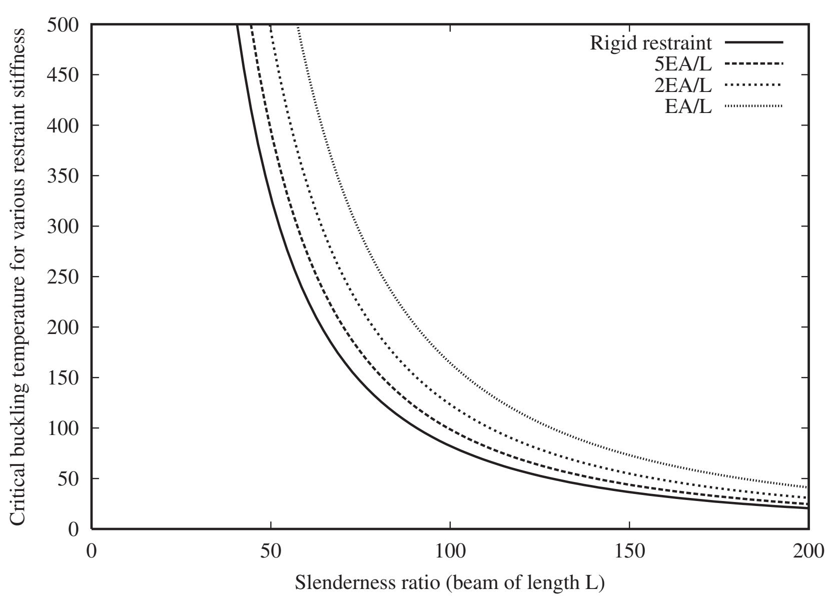

Fig. 5. Buckling temperatures for thermal expansion against finite lateral restraint.

Relationships can be derived for thermal bowing analogous to the ones derived earlier for thermal expansion. Figure 6 shows a beam subjected to a uniform temperature gradient through its depth d along its whole length. Assuming the beam is simply supported (as shown in Figure 6) we can derive the following relationships:

1. The thermal gradient, $T_{,y}$, over the depth is $\dfrac{T_2 - T_1}{d}$
2. A uniform curvature $\phi = \alpha\, T_{,y}$ is induced along the length as a result of the thermal gradient
3. Due to the curvature of the beam the horizontal distance between the ends of the beam will reduce. If this reduction is interpreted as a contraction strain, ε_ϕ, analogous to the thermal expansion strain ε_T mentioned earlier, the value of this strain can be calculated from analyzing Figure 6 as

$$\varepsilon_\phi = 1 - \frac{\sin\dfrac{l\phi}{2}}{\dfrac{l\phi}{2}} \tag{8}$$

Now consider the laterally restrained beam of Figure 3. If a uniform thermal gradient, $T_{,y}$, without any average rise in temperature, is applied to this beam, as shown in Figure 7, the result is a thermally induced tension in the beam and corresponding reactions at the support (opposite to the pure thermal expansion case discussed earlier). This is clearly caused by the restraint to end translation against the contraction strain, ε_ϕ, induced by the thermal gradient.

Figure 8 shows a fixed-end beam (by adding end rotational restraints to the beam of Figure 7) subjected to a uniform temperature gradient through its depth. Recalling that a uniform curvature $\phi = \alpha T_{,y}$ exists in a simply supported beam subjected to gradient $T_{,y}$; if that beam is rotationally restrained by support moments, M, uniform along its length, an equal and opposite curvature induced by the support moments cancels out the thermal curvature and therefore the fixed-end beam remains straight with a constant moment $M = EI\phi$ along its length.

From the above discussion it is clear that the effect of boundary restraints is crucial in determining the response of structural members to thermal actions. The key conclusion to be drawn from the discussion so far is that thermal strains will be manifested as displacements if they are unrestrained or as stresses if they are restrained through counteracting mechanical strains generated by restraining forces.

As discussed earlier for lateral restraint, perfect rotational restraint is also not very easily achieved in real structures (other than for symmetric loading on members over continuous supports, without any *hinges* from strength degradation). Figure 9 shows a beam restrained rotationally at the ends by rotational springs of stiffness k_r. In this case the restraining moment in the springs as a result of a uniform thermal

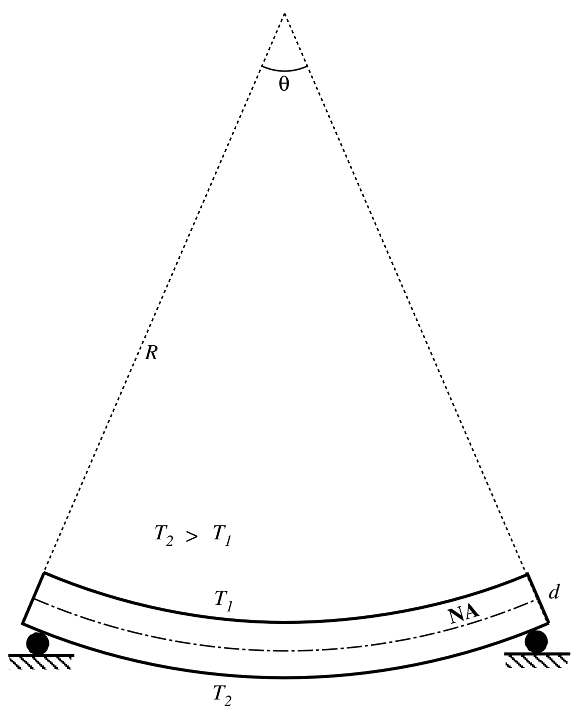

Fig. 6. Simply supported beam subjected to a uniform thermal gradient.

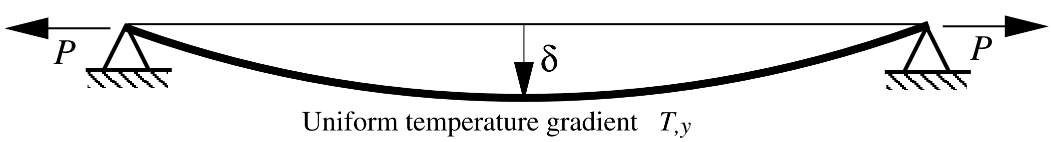

Fig. 7. Laterally restrained beam subjected to a uniform thermal gradient.

gradient $T_{,y}$ can be found to be,

$$M = \frac{EI\alpha T_{,y}}{1 + \frac{2EI}{k_r l}} \tag{9}$$

This equation implies that if the rotational restraint stiffness is equal to the rotational stiffness of the beam itself, *EI*/*l*, then the moment it will attract will be about one-third of a fixed support moment.

Combinations of Thermal Expansion and Thermal Bowing

In the previous sections the response of beams to either thermal expansion or thermal bowing has been considered in isolation. To study the combined response let us first consider the case of a fixed-end beam as shown in Figure 10, which is both rotationally and translationally restrained at both ends. If this beam is subjected to a mean temperature rise and a through depth thermal gradient, it will experience a uniform compressive stress because of restrained expansion and a uniform moment because of the thermal gradient. The stresses on any typical cross section because of the combined effect of the two thermal actions are also shown in Figure 10.

Fig. 8. Fixed-end beam subjected to a uniform thermal gradient.

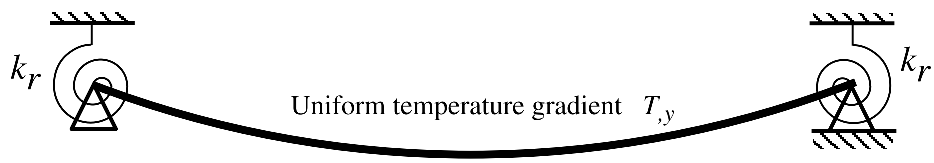

Fig. 9. Beam with finite rotational restraint with a uniform thermal gradient.

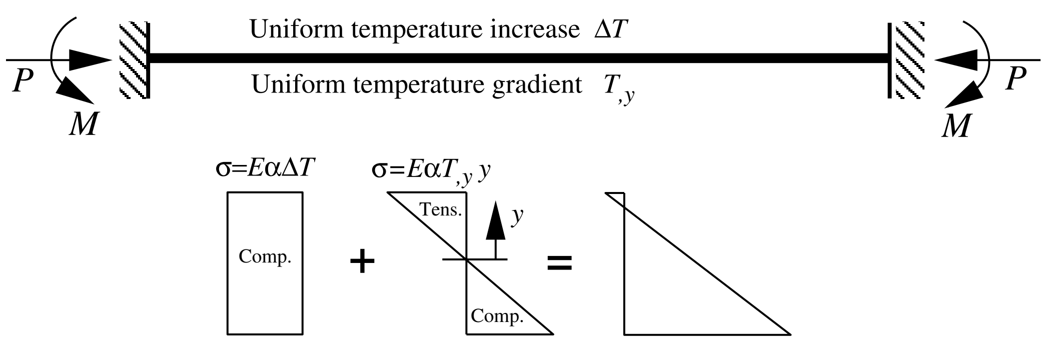

Fig. 10. Combined thermal expansion and bowing in a fixed-end beam.

It is clear that the bottom of the beam will experience very high compressive stresses, while the top may be anywhere between significant compression to significant tension.

The above scenario is a common one in composite frame structures such as Cardington. The composite action of a steel beam framing into an interior column with a continuous slab over it, produces conditions very close to a fully-fixed support (as in Figure 10). The high compressions resulting from the combined effect of thermal actions as described above almost invariably produce local buckling in the lower flange of the steel beam very early on in a fire. This is why local buckling of the lower flanges is such a common occurrence in fires, as seen in all Cardington tests (Martin and Moore, 1997) and other fires (Steel Construction Institute, 1991).

Once local buckling has occurred, the pattern of stresses at the ends of the composite beam changes. The end negative moment in the composite section (tension at the top of the concrete slab and compression in the steel beam), referred to as *hogging moment* in the United Kingdom (as opposed to *sagging* moment in the span), is relieved by the *hinge* produced by local buckling and the end restraint conditions change to the one shown in Figure 7. As this happens quite early in real fires, the end conditions described by Figure 7 are the ones that govern the behavior of a composite beam for the best part of the fire.

The fundamental pattern of behavior of a beam whose ends are laterally restrained (but rotationally unrestrained, see Figure 7) subjected to thermal expansion and thermal bowing separately, was established in previous sections. Restrained expansion resulted in compression and bowing resulted in tension. This helped to illustrate that two opposite stress regimes can occur depending upon the thermal regime applied, however the apparent response of the beam is the same (in other words, downward deflection). The main parameters that determine the response are an average temperature equivalent rise, ΔT, and an average equivalent thermal gradient, $T_{,y}$. For practical application of the expressions presented in this paper, these parameters must first be determined. A procedure for determining these values in beams of any general cross section with any temperature distribution over the depth is given in Usmani and Lamont (2002).

To study the effects of applying combinations of thermal expansion and thermal bowing, define an effective strain as follows:

$$\varepsilon_{eff} = \varepsilon_T - \varepsilon_\phi \qquad (10)$$

Positive values of ε_{eff} imply compression (or the effect of mean temperature rise is dominant) and negative values imply tension (or the effect of thermal gradients is dominant). The variation of ε_{eff} for various thermal regimes can produce a large variety of responses as shown in Figure 11.

From the discussion above, a simple criterion for all the various types of responses observed can be developed. If ε_{eff} is close to π^2/λ^2, then there will be no buckling as not enough compression is generated. A dimensionless number ζ may be defined as follows to categorize the various responses:

$$\zeta = \frac{\varepsilon_T - \varepsilon_\phi}{\dfrac{\pi^2}{\lambda^2}} \qquad (11)$$

To summarize:

1. $\zeta >> 1$ typically generates pre- and post-buckling type deflection responses with thermal expansion and compression dominant. The compression force patterns are as discussed earlier in the restrained thermal expansion section.

2. $\zeta \approx 1$ generates responses where most of the thermal expansion is converted into deflection but there are negligible stresses in the beam.

3. $\zeta << 1$ generates a thermal bowing dominated response with deflection patterns similar to the *zero stress* pattern in Figure 11, with considerable tensile forces in the beam, which grow with the increase in the gradient.

Summary of the Key Points So Far

To allow for transparency and simplicity, all the discussion so far has used a simple beam model; however, the concepts presented are very general in nature and can be used very effectively in interpreting the behavior of much more complex structures. A summary of the key points is presented here for such a purpose.

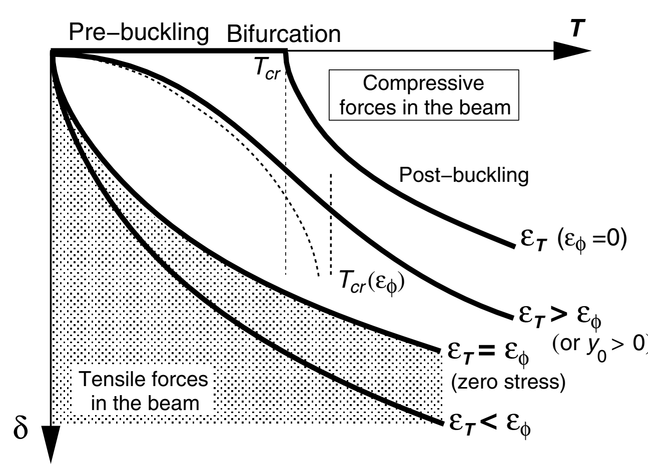

Fig. 11. Temperature deflection responses for combinations of ε_T and ε_ϕ.

1. Unrestrained thermal expansion caused by a rise in mean temperature causes ends to move apart. The thermal strain producing this expansion is $\varepsilon_T = \alpha\Delta T$.

2. Thermal expansion in the presence of restraint to lateral translation from the surrounding structure produces compression forces leading to yielding or buckling (both the restraint and the temperature rise do not have to be large for buckling or yielding to occur).

3. Thermal bowing caused by the through depth thermal gradient leads to curvature $\phi = \alpha T_{,y}$. The thermally-induced curvature results in *pulling in* of the ends in a simply-supported beam. The measure of reduction in distance between the ends can be written as a *contraction strain*

$$\varepsilon_\phi = 1 - \frac{\sin {}^{l\phi}\!/_{2}}{{}^{l\phi}\!/_{2}}$$

4. Restraint to end translation produces tensions in the beam, which increase with growth in the thermal gradients.

5. Rigid restraint to end rotation produces a hogging moment of $EI\phi$ over the whole length of the beam with no curvature. Finite rotational restraints produce combinations of hogging moments and curvature.

6. Compatibility of displacements in compartments with orthogonal stiffness distribution and orthogonal temperature distribution (or simply compartments with an aspect ratio significantly different from unity) influences the forces and displacements in the members.

These basic principles are indispensable in analyzing the often confusing and voluminous output data from computational models or experiments, such as the Cardington tests.

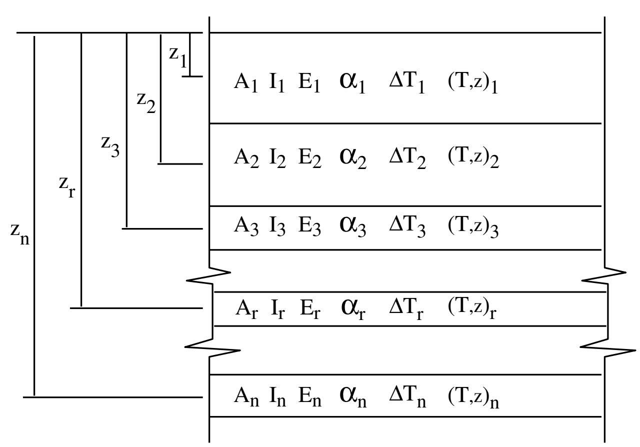

Fig. 12. A general composite section divided into n *slices.*

Estimation of Equivalent Temperature Effects on the Model

Given that the cross sections of composite structural members and the temperature distributions over their depths can be quite complicated, the issue of equivalent thermal loading that must be applied to the members is not straightforward. A procedure has been developed based upon ideas used in estimating the effects of thermally induced stresses in bridge decks (Johnson and Buckby, 1986).

Figure 12 shows a general composite section with the indicated properties and temperature conditions, as defined by a uniform temperature increment, ΔT_r, and a through-depth thermal gradient, $(T_{,z})_r$, for a given slice, r. If the beam that the section belongs to is fully restrained (for both end translations and end rotations) then each slice will have a force and moment associated with it, defined as

$$F_r = E_r A_r \alpha_r \Delta T_r = E_r A_r (\varepsilon_T)_r = E_{max} \hat{A}_r (\varepsilon_T)_r \tag{12}$$

and

$$M_r = E_r I_r \alpha_r (T_{,z})_r = E_{max} \hat{I}_r \phi_r \tag{13}$$

It is convenient to write the above quantities using a transformed area, by defining modular ratios m_r based on the highest modulus in the composite section; this is what $\hat{A}_r$ and $\hat{I}_r$ represent. The resultant force, $\bar{F}$, and resultant moment, $\bar{M}$, can now be determined from

$$\bar{M} + \bar{F}\bar{z} = \sum F_r z_r + \sum M_r \tag{14}$$

where

$\bar{z}$ = centroid of the composite section

If the total transformed area and second moment of area of the composite are denoted by $\bar{A}$ and $\bar{I}$, then the equivalent expansion, $\bar{\varepsilon}_T$, and curvature, $\bar{\phi}$, can be written as

$$\bar{\varepsilon}_T = \frac{\bar{F}}{E_{\max} A} \tag{15}$$

and

$$\bar{\phi} = \frac{\bar{M}}{E_{\max} I} \tag{16}$$

This procedure can also be used to determine the thermally induced strains and stresses in a composite beam. This can be done by releasing the restraint applied to determine the resultant force and moment in the composite section; which, of course, is the same as applying the negatives of $\bar{F}$ and $\bar{M}$ in order to reduce the restraint forces to zero. This is illustrated using an example in Figure 13. The total strain distribution in the beam can then be determined by,

$$\varepsilon(z) = \bar{\varepsilon}_T + (z - \bar{z})\bar{\phi} \tag{17}$$

$$\sigma(z) = \frac{E_{\max}}{m_r}\left[\left(\bar{\varepsilon}_T\right)_r + (z - z_r)\phi_r + \varepsilon(z)\right] \tag{18}$$

Figure 13 shows the distributions of stresses and strains computed using this procedure for a simple example of a composite beam.

THE PHENOMENON OF LOCAL BUCKLING OF STEEL BEAMS IN COMPOSITE ACTION WITH CONCRETE SLABS

The first significant event that occurs when a composite steel frame structure is subjected to fire is local buckling of the bottom flange of the steel beam (particularly if these are not fire protected). The explanation of this phenomenon is quite simple keeping in mind the end restraint conditions of the composite beams (as shown in Figure 14) and provides an excellent practical illustration of the principles presented earlier.

As the temperature in the compartment increases, there are three cumulative effects that contribute toward the increase in compressive stresses along the steel beam bottom flange. The first of these is the load itself, which produces an initial hogging moment, leading to compression at the beam bottom flange. The second is the increasing mean temperature of the composite beam leading to overall compression across the equivalent composite section. Finally the thermal gradient over the depth of the section (cool slab and hot steel) leads to a uniform hogging moment developing along the length of the section, again leading to compression in the steel bottom flange. So the stress at the bottom flange of the steel beam may be written as:

$$\sigma(z) = \frac{M_w z}{I} + E_{\max}\alpha\Delta T + E_{\max}\bar{\phi}z \tag{19}$$

where

M_w = fixed-end moment from the uniformly distributed load, w

z = distance from the centroid

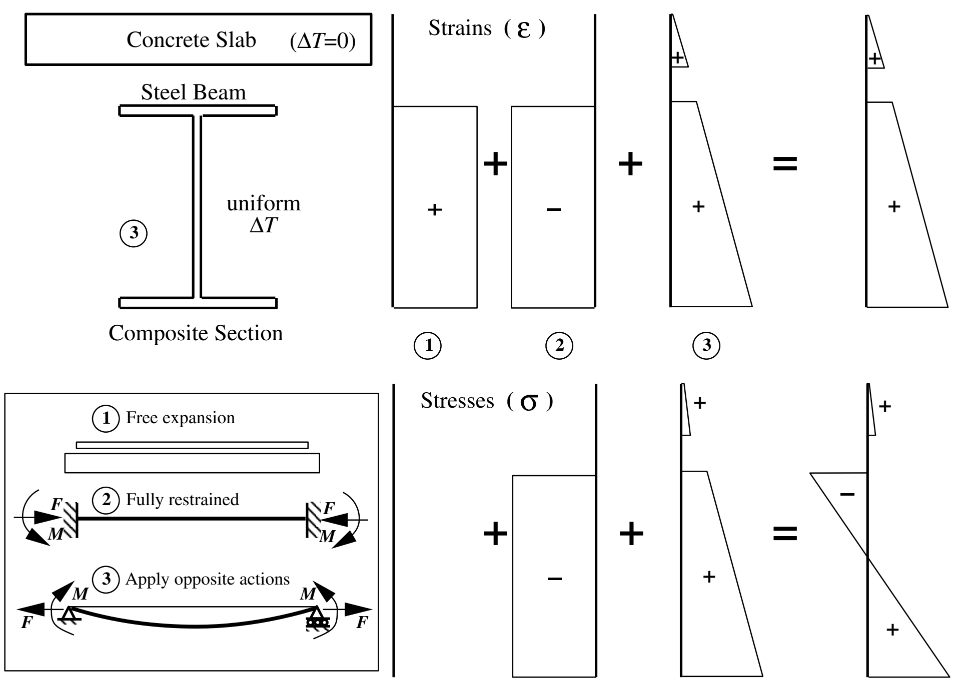

Fig. 13. Analysis of thermal actions on a composite beam.

As the temperature goes on increasing, the overall compression in the composite beam increases as well as the overall hogging moment and the stress at the beam bottom flange rises steadily, until this stress exceeds the local buckling (or yielding) stress. At this point the local buckling changes the composite end conditions so that end rotations may take place, and therefore the increase in growth of axial force in the composite stabilizes (to a plateau), because the thermal expansion can now be absorbed into the increasing deflections instead of increasing compression.

To examine this event in detail, let us consider the composite secondary beam from the Cardington restrained beam test. Figures 15 and 16 show the layout of the test and the active structural sections spanning in the two directions. Table 1 shows the equivalent section properties for the two directions.

For the composite beam section temperatures and gradients were calculated for three different reference temperature states of the steel beam, for both directions (longitudinal and transverse), using the procedure outlined earlier. The results

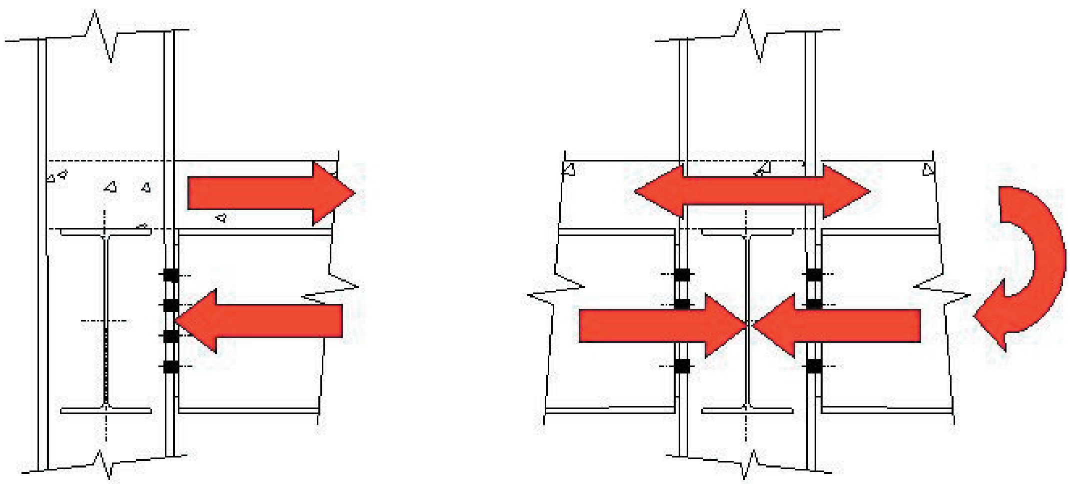

Fig. 14. Typical end restraint conditions for composite members.

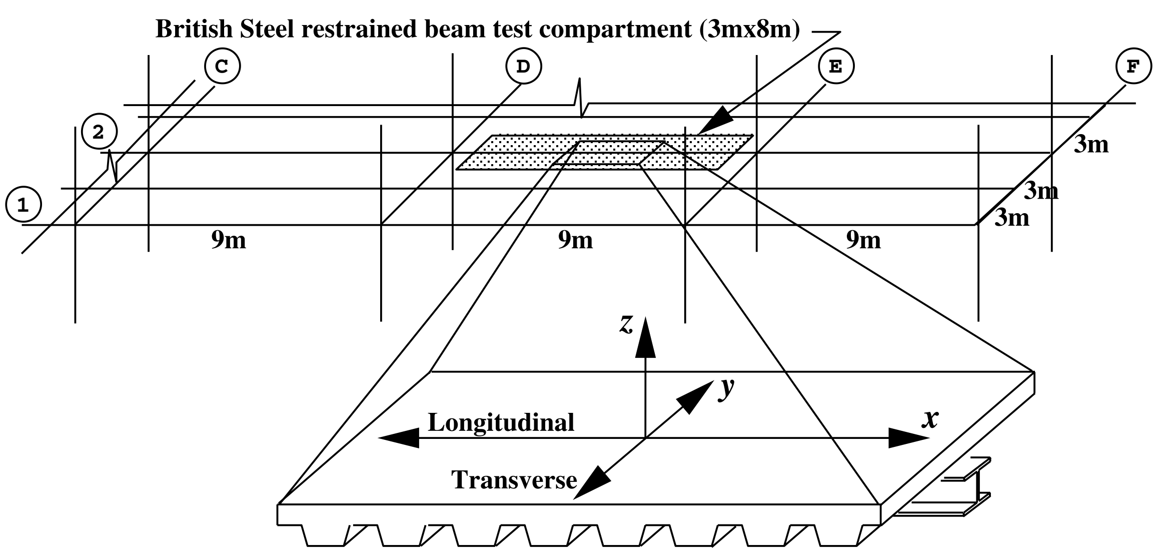

Fig. 15. Layout of the restrained beam test at Cardington.

Table 1. Section Properties of Composite Slab in *x* and *y* Directions					
	Area, *A* mm^2	Second Moment of Area, *I* mm^4	Depth of Centroid, $\bar{z}$ mm	Modulus, *E* kN/ mm^2	Coeff. of Thermal Expansion, α $^oC^{-1}$
x-Slab	157500	$257x10^6$	35	7.5	$8x10^{-6}$
Steel beam	5150	$85x10^6$	282	200	$12x10^{-6}$
x-Composite	10900	$250x10^6$	148	200	$10x10^{-6}$
y-Slab (1 rib)	30700	$38x10^6$	55	7.5	$8x10^{-6}$

are tabulated in Tables 2a and 2b, along with other data that will be used in the analysis. It may be noted that the temperature distributions in the real structure are complicated by the effect of the ribs, and therefore appropriate averages have been used in these calculations. λ denotes slenderness ratio, and $\bar{z}$ denotes the depth of centroid of the transformed composite sections, subscripts *x* and *y* have been used to indicate longitudinal or transverse directions. Most other quantities in the tables should be self-explanatory.

Previous analysis (Usmani, 2000) has shown that for this test rigid restraint to end translation may be safely assumed. Also, Usmani and others (2001) have indicated that restraint stiffness may not have to be very large for most of these phenomena to be observed. Therefore, assuming rigid restraint to end translation for the composite beam, the stress in the bottom flange at 150 °C (302 °F) is calculated as 573 MPa (83.1 ksi) [127 MPa (18.4 ksi) from the uniformly distributed load of 16.5 kN/m (1.13 kip/ft), 160 MPa (23.2 ksi) from the equivalent mean temperature rise over the composite, and 286 MPa (41.5 ksi) from the equivalent thermal gradient over the depth]. This exceeds the reported maximum yield stress of the steel [318 MPa (46.1 ksi)] and the flange would certainly have buckled at a temperature lower than this. It is interesting to note that the thermal bowing contribution

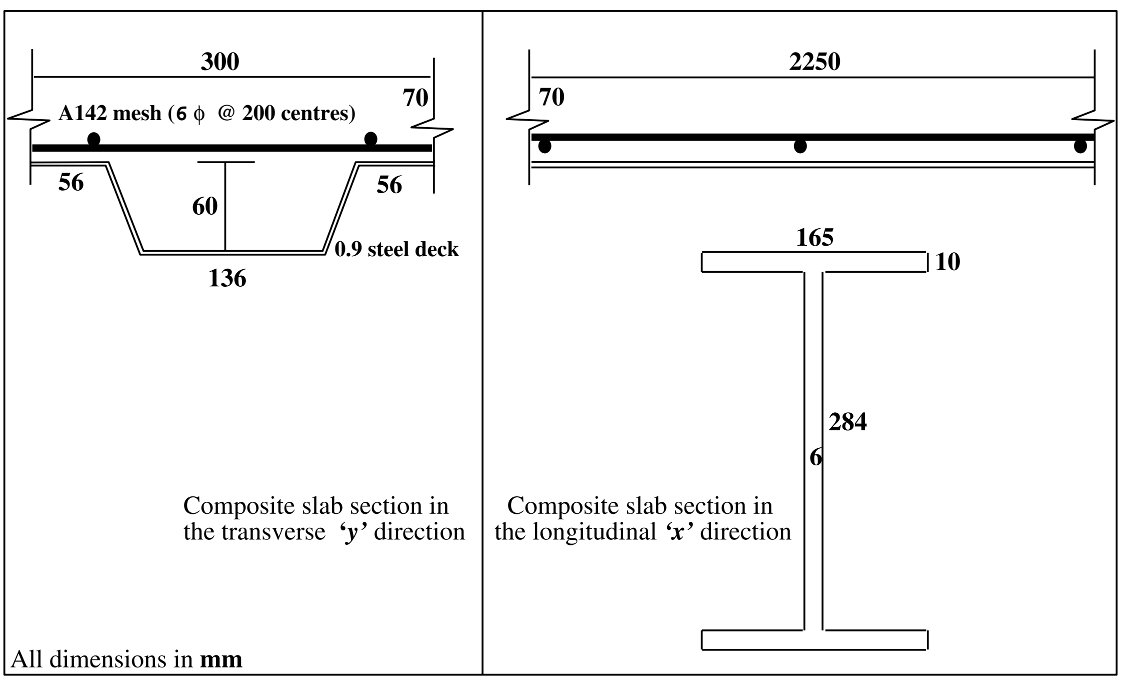

Fig. 16. Active composite cross sections in x *and* y *directions.*

Table 2a. Properties of Composite Slab in x Direction at Different Temperatures

Steel Temperature	E_s kN/mm^2 (ksi)	E_c kN/mm^2 (ksi)	A_x mm^2 (in.^{2})	I_x mm^4 (in.^{4})	$\bar{z}_x$ mm (in.)	λ_x	ΔT_x °C (°F)	$(T_{,z})_x$ °C/mm (°F/in.)
150 °C (302 °F)	200.0 (29,000)	7.5 (1090)	10900.0 (16.9)	250x10^6 (600)	148.0 (5.8)	60	80 (140)	0.5 (55)
500 °C (932 °F)	100.0 (14500)	7.5 (1090)	16800.0 (26.0)	300x10^6 (721)	108.5 (4.3)	67	260 (470)	1.6 (110)
800 °C (1470 °F)	0.0 0.0	7.0 (1020)	124000 (192)	48x10^6 (115)	30.0 (1.2)	450	240 (430)	5.0 (260)

Table 2b. Properties of Composite Slab in y Direction at Different Temperatures

Steel Temperature	E_c kN/mm^2 (ksi)	A_y mm^2 (in.^{2})	I_y mm^4 (in.^{4})	$\bar{z}_y$ mm (in.)	λ_y	ΔT_y °C (°F)	$(T_{,z})_y$ °C/mm (°F/in.)
150 °C (302 °F)	7.5 (1090)	30700.0 (47.6)	38x10^6 (91.3)	55.0 (2.17)	170	- (-)	- (-)
500 °C (932 °F)	7.5 (1090)	30000.0 (46.5)	37x10^6 (88.9)	54.5 (2.15)	170	85 (153)	1.4 (96)
800 °C (1470 °F)	7.5 (1090)	19200.0 (29.8)	17x10^6 (40.8)	39.0 (1.54)	200	250 (450)	4.8 (250)

is the greatest to local buckling. Therefore, one may expect this phenomenon to occur earlier (at lower temperatures) in short hot fires (with larger gradients) than in long cool fires (with larger mean temperatures). The local buckling stress for an I-section in bending can be approximately calculated by Trahair and Bradford (1998).

$$\sigma_{cr} = \frac{\pi^2 E}{12(1-\nu^2)} \frac{0.425}{\left(b_f / t_f\right)^2} \tag{20}$$

where

ν = Poisson's ratio
b_f = half the overall flange width
t_f = flange thickness

This equation produces a very large value of buckling stress, suggesting that the local buckle observed must have actually occurred at the yield stress, which occurred at approximately 120 °C (248 °F) based on the test results (Sanad and others, 2000c).

BEHAVIOR OF COMPOSITE FLOOR SYSTEMS

For clarity of illustration, of the most fundamental concepts so far, only the behavior of beams within a plane has been considered. However it is clear that floor systems will act in at least two orthogonal directions and the compatibility constraints are likely to have a significant effect on overall behavior. The greater the difference between the two directions the more significant this effect becomes. The Cardington restrained beam test (geometry illustrated in Figure 15) provides a good example of this phenomenon, as the dimensions of the fire compartment for this test are 8 m × 3 m (26 ft × 9.8 ft) (an aspect ratio of more than 2). From first principles, it is clear that the longer span of 8 m will expand considerably more than the shorter 3 m span. This would occur even if the structural material properties of the two spans were identical. In this case, however, there are other

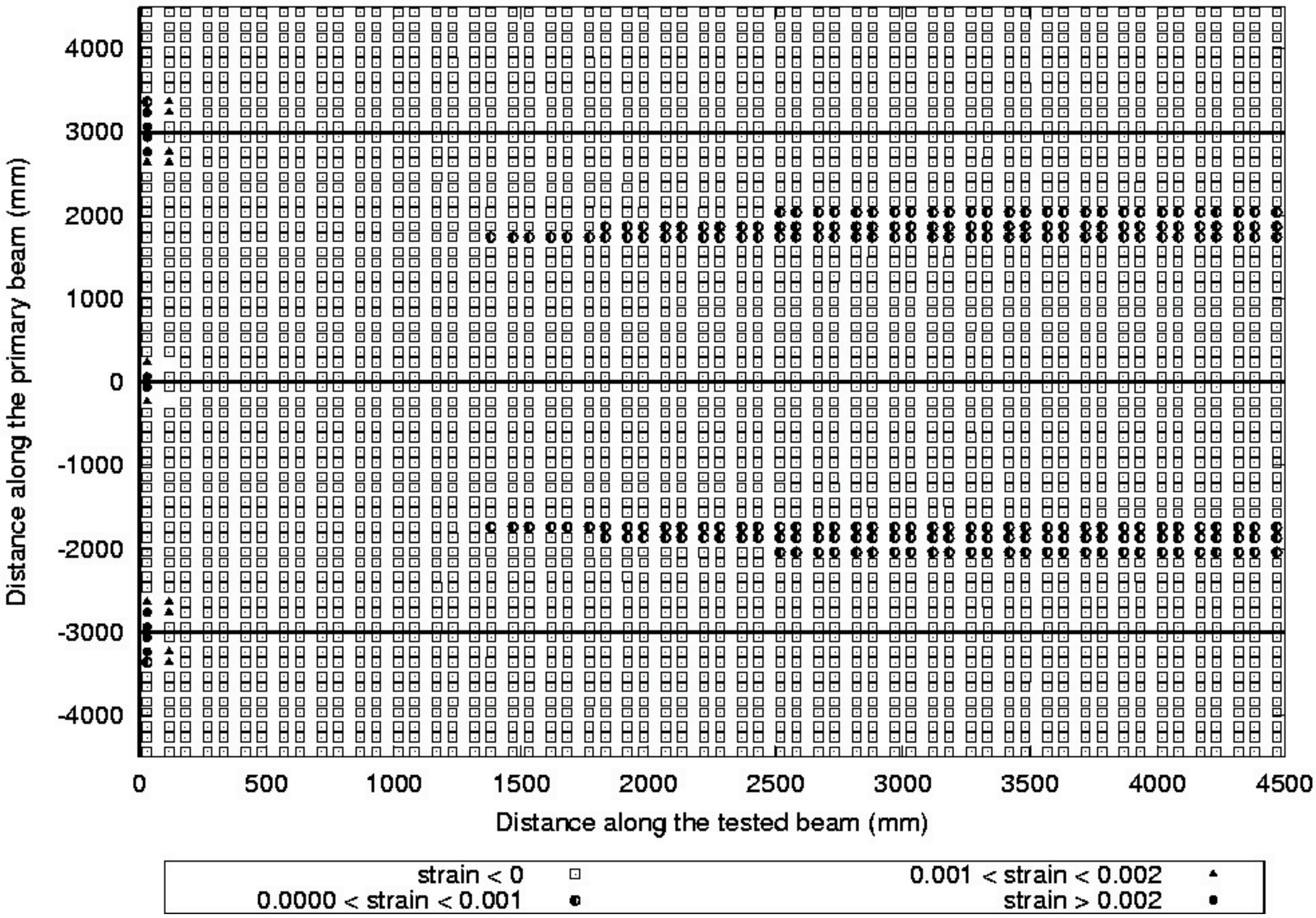

Fig. 17. Reinforcement level longitudinal strain patterns in the restrained beam.

differences, the long span has an unprotected steel beam in composite action with the concrete slab and the short span has the slab profile (ribs). The much greater thermal expansion in the long span (which is quite rigidly restrained by the surrounding structure) will make it want to deflect considerably more than the short span will allow (because of the compatibility requirement). This will induce an even larger compression force in the long span than restrained thermal expansion alone. In the short span, a large tension force will be generated, as the long span will decrease the tension force. A simple analysis (Usmani, 2000) based on the basic ideas presented in this paper shows this clearly. A more rigorous analysis carried out using the software ABAQUS shows this effect conclusively (Gillie and others, 2001). Figure 17 shows strains in the slab at reinforcement level in the restrained beam test in the longitudinal direction (at the end of heating) which are practically all compressive. The strains in the transverse direction (Figure 18) show compressions in the low deflection regions, near the ends of the compartment, and tensions in the large deflection region near midspan. In this case of a highly restrained system, the tensions are not caused by the loading, but by the compatibility requirements of a large aspect ratio (8:3) compartment.

For compartments with more even spans, the whole floor system may be in compression to begin with. The compressive stresses developing in concrete enhance its load carrying capacity, similar to prestressing. This effect depends upon three factors: a) restraint: in regions where the restraint to expansion is high; b) location: in low deflection regions where the thermal strains are unable to be absorbed in deflections, such as regions near the support boundaries; c) fire scenario: a short hot fire will cause larger gradients and lower compression or tension forces while a longer cooler fire will produce higher mean temperatures and therefore greater compression forces against restraints. A good illustration of the ideas presented earlier, when the combined (opposite) effect of mean temperatures and through depth thermal gradients was discussed, is shown in Figure 19. This figure shows a calculation of the effective strain, ε_{eff}, in one of the Cardington fire tests (British Steel Corner Test), which had a relatively even aspect ratio [8 m × 10 m (26 ft × 33 ft)]. The effective mechanical strain variation over the depths of

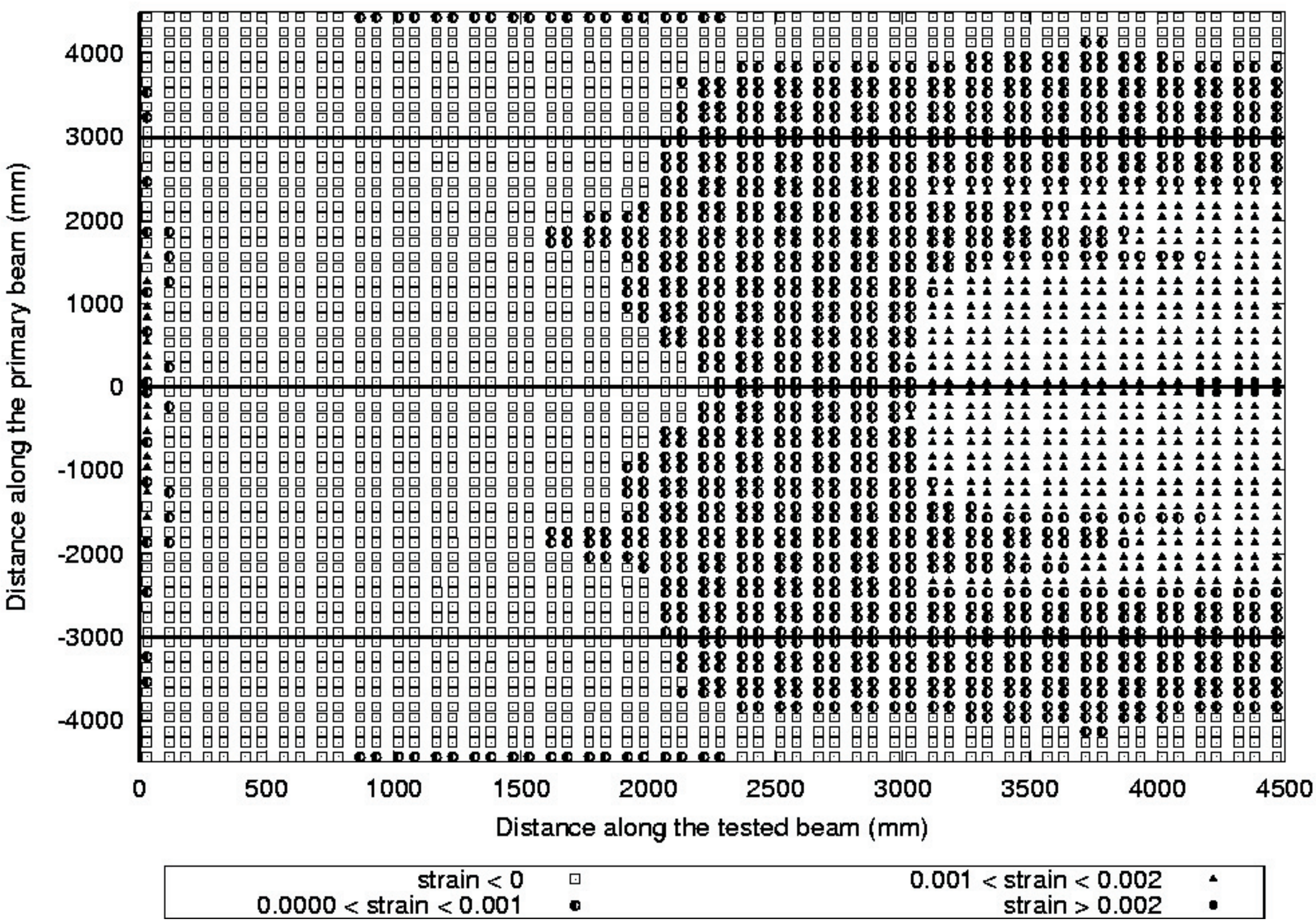

Fig. 18. Reinforcement level transverse strain patterns in the restrained beam.

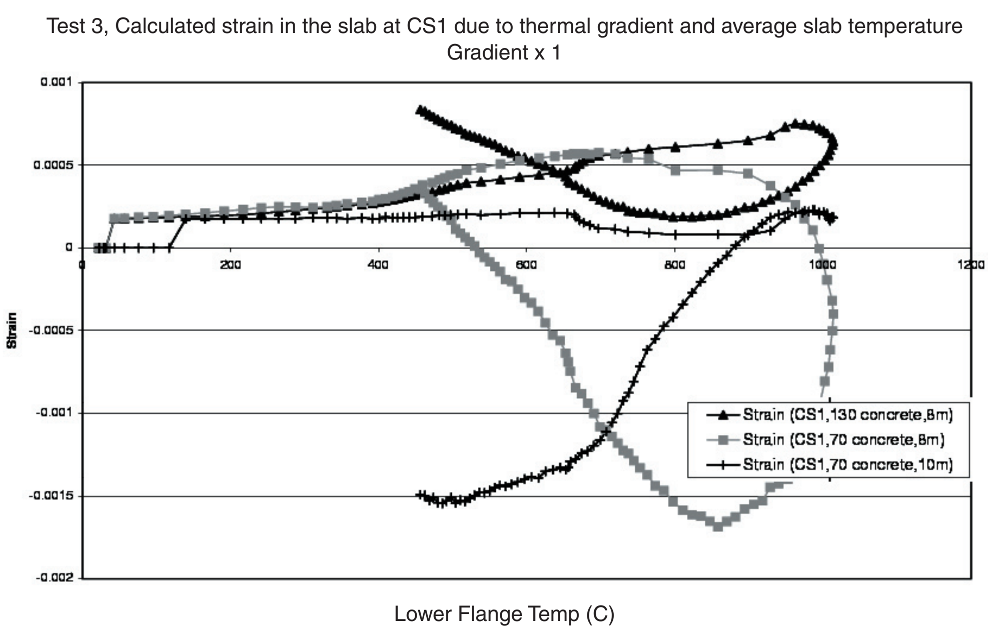

Fig. 19. Effective strain ε_{eff} in the concrete slab of the British Steel Corner Test.

the profiled concrete slab is shown for both spans against the unprotected steel temperature. It can be seen that these strains are very low all the way through the fire and they are all in compression, even though at the end of the fire the middle region of the floor had deflections of around 400 mm (16 in.) and all internal beams which were unprotected were exposed to a fire of over 1000 °C (1832 °F) for over an hour. Therefore the floor system and the structure as a whole were nowhere near failure.

In the later stages of the fire (assuming it is hot enough and goes on for long enough) the accumulated thermal strains will have made the floor system sag considerably. This however is just the geometric form that allows it to continue carrying the loads in tensile membrane action (see Figure 20) in preference to the flexure mechanism (which has degraded because of the loss of the composite steel and concrete material properties). The reinforcing mesh will continue to provide reliable tensile membrane capacity given that it is sufficiently anchored at the boundaries and is continuous (sufficiently lapped) within the spans. A detailed analysis and design method has been developed for composite floor systems, an early version of which will be published soon (Usmani and Cameron, 2004).

SUMMARY

This paper provides a brief and incomplete account of the mechanics of structural response to fire. The emphasis has been on describing the behavior of floor systems; however most of the ideas extend to columns as well. The main difference is that floor systems can generally remain stable for long periods by adopting alternative load carrying paths and this behavior can be exploited in design to achieve greater robustness and economy. Columns on the other hand must always be fire protected. The interactions between the floor system and the columns (exterior columns in particular) can be of critical importance in understanding *whole structure* behavior.

The paper shows that the key factor determining structural response to fires is how thermal strains induced in its members are accommodated. These strains take the form of thermal expansion (under an average centroidal temperature rise) and curvature (induced by a temperature gradient through the section depth). If the structure has insufficient end translational restraint to thermal expansion, the strains are taken up in expansive displacements. Thermal gradients induce curvature leading to *bowing* of a member whose ends are free to rotate.

Members whose ends are restrained against translation produce opposing mechanical strains to thermal expansion strains and therefore large compressive stresses. Curvature strains induced by the thermal gradient in members whose ends are rotationally restrained can lead to large hogging (negative) bending moments throughout the length of the member without deflection. The effect of induced curvature in members whose ends are rotationally unrestrained, but translationally restrained, is to produce tension.

For the same deflection in a structural member, a large variety of stress states can exist: large compressions where restrained thermal expansion is dominant; very low stresses where the expansion and bowing effects balance each other; in cases where thermal bowing dominates, tension occurs in laterally-restrained and rotationally-unrestrained mem-

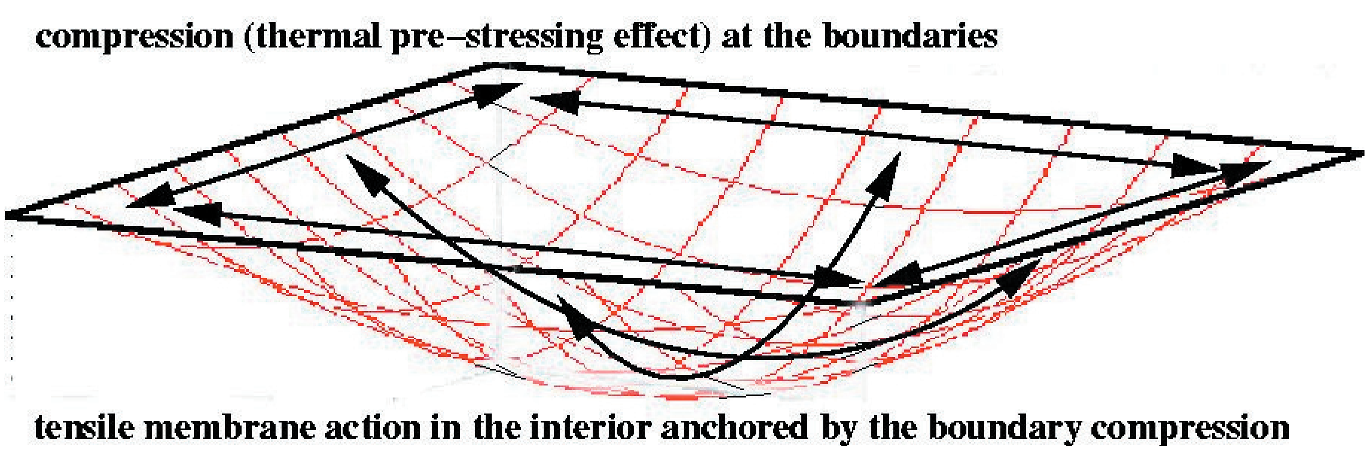

Fig. 20. Tensile membrane behavior in spans and thermal pre-stressing at boundaries.

bers, while large hogging moments occur in rotationally restrained members. This variety of responses can indeed exist in real structures if one imagines the many different types of fire a structure may be subjected to. A fast burning fire that reaches flash-over and high temperatures quickly and then dies off can produce high thermal gradients (hot steel and relatively cold concrete) but lower mean temperatures. By contrast, a slow fire that reaches only modest temperatures but burns for a long time could produce considerably higher mean temperature and lower thermal gradients.

Most situations in real structures under fire have a complex mix of mechanical strains due to applied loading and mechanical strains due to restrained thermal expansion. These lead to combined mechanical strains which often far exceed the yield values, resulting in extensive plastification. The deflections of the structure, by contrast, depend only on the total strains, so these may be quite small where high restraint exists, but they are associated with extensive plastic straining. Alternatively, where less restraint exists, larger deflections may develop, but with a lesser demand for plastic straining and less destruction of the stiffness and strength properties of the materials.

The final message from this paper is that the behavior of steel-framed composite structures in fire is sufficiently well understood now to enable the development of new design methods. These methods should be based on the concepts of the limit state design within an appropriate risk and reliability framework.

REFERENCES

Gillie, M., Usmani, A.S., and Rotter, J.M. (2001), "Structural Analysis of the First Cardington Test," *Journal of Constructional Steel Research*, Vol. 57, pp. 581-601, United Kingdom.

Gillie, M., Usmani, A.S., and Rotter, J.M. (2002), "A Structural Analysis of the Cardington British Steel Corner Test, *Journal of Constructional Steel Research*, Vol. 58, pp. 427-443, United Kingdom.

Johnson, R.P. and Buckby, R.J. (1986), "Composite Structures of Steel and Concrete—Volume 2: Bridges," Collins, London, United Kingdom.

Lamont, S. and Usmani, A.S. (2003), "Possible Panel Instability in Composite Deck Floor Systems under Fire," *Journal of Constructional Steel Research*, Vol. 59, pp. 1397-1433, United Kingdom.

Lamont, S., Lane, B., Usmani, A.S., and Drysdale, D.D. (2002), "Assessment of the Fire Resistance Test with Respect to Beams in Real Structures," American Institute of Steel Construction, Inc., *Engineering Journal*, Vol. 40, No. 2, pp. 63-75, Chicago.

Martin, D.M. and Moore, D.B. (1997), "Introduction and Background to the Research Program and Major Fire Tests at BRE Cardington," *National Steel Construction Conference Proceedings*, pp. 37-64, May.

Sanad, A.M., Lamont, S., Usmani, A.S., and Rotter, J.M. (2000a), "Structural Behaviour in a Fire Compartment Under Different Heating Regimes—Part 1 (Slab Thermal Gradients)," *Fire Safety Journal*, Vol. 35, pp. 99-116, United Kingdom.

Sanad, A.M., Lamont, S., Usmani, A.S. and Rotter, J.M. (2000b), "Structural Behaviour in a Fire Compartment Under Different Heating Regimes—Part 2 (Slab Mean Temperatures)," *Fire Safety Journal*, Vol. 35, pp. 117-130, United Kingdom.

Sanad, A.M., Rotter, J.M., Usmani, A.S., and O'Connor, M. (2000c), "Composite Beam in Buildings Under Fire," *Fire Safety Journal*, Vol. 35, pp. 165-188, United Kingdom.

Steel Construction Institute (1991), "Structural Fire Engineering Investigation of Broadgate Phase 8 Fire," Technical Report, Steel Construction Institute, Ascot, United Kingdom.

Trahair, N.S. and Bradford, M.A. (1998), "The Behaviour and Design of Steel Structures to AS 4100," E. & F.N. Spon, London, United Kingdom.

University of Edinburgh (2000), *Behaviour of Steel Framed Structures under Fire Conditions*, Technical Report Main Report, DETR-PIT Project, School of Civil and Environmental Engineering, University of Edinburgh, United Kingdom, http://www.civ.ed.ac.uk/research/fire/technicalreports.html.

Usmani, A.S. (2000), "Application of Fundamental Structural Mechanics Principles in Assessing the Cardington Restrained Beam Test," *Technical Report TM4*, DETR-PIT Project, School of Civil and Environmental Engineering, University of Edinburgh, http://www.civ.ed.ac.uk/research/fire/technicalreports.html.

Usmani, A.S. and Cameron, N. (2004), "Limit Capacity of Composite Floor Slabs in Fire," *Cement and Concrete Composites Journal*, Vol. 26, pp. 127-140.

Usmani, A.S., Chung, Y.C., and Torero, J.L. (2003), "How Did the WTC Towers Collapse? A New Theory," *Fire Safety Journal*, Vol. 38, pp. 501-533, United Kingdom.

Usmani, A.S., Rotter, J.M., Lamont, S., Sanad, A.M., and Gillie, M. (2001), "Fundamental Principles of Structural Behaviour under Thermal Effects," *Fire Safety Journal*, Vol. 36, pp. 721-744, United Kingdom.

Usmani, A.S. and Lamont, S. (2002), "Key Events in the Structural Response of a Composite Steel Frame Structure in Fire," *Proceedings of the SiF'02, The Second International Workshop for Structures in Fire*, pp. 351-368, Christchurch, New Zealand, March.